Nanoscale Advances

ROYAL SOCIETY OF CHEMISTRY

PAPER

View Article Online
View Journal | View Issue

Cite this: *Nanoscale Adv.*, 2023, **5**, 2813

Magnetic order and magnetic anisotropy in two-dimensional ilmenenes†

R. H. Aguilera-del-Toro, [ab] M. Arruabarrena,[b] A. Leonardo[ac] and A. Ayuela *[ab]

Received 2nd March 2023
Accepted 10th April 2023

DOI: 10.1039/d3na00134b

rsc.li/nanoscale-advances

Iron ilmenene is a new two-dimensional material that has recently been exfoliated from the naturally occurring iron titanate found in ilmenite ore, a material that is abundant on the earth's surface. In this work, we theoretically investigate the structural, electronic and magnetic properties of 2D transition-metal-based ilmenene-like titanates. The study of magnetic order reveals that these ilmenenes usually present intrinsic antiferromagnetic coupling between the 3d magnetic metals decorating both sides of the Ti–O layer. Furthermore, the ilmenenes based on late 3d brass metals, such as $CuTiO_3$ and $ZnTiO_3$, become ferromagnetic and spin compensated, respectively. Our calculations which include spin–orbit coupling reveal that the magnetic ilmenenes have large magnetocrystalline anisotropy energies when the 3d shell departs from being either filled or half-filled, with their spin orientation being out-of-plane for elements below half-filling of 3d states and in-plane above. These interesting magnetic properties of ilmenenes make them useful for future spintronic applications because they could be synthesized as already realized in the iron case.

1 Introduction

Technology for synthesizing two-dimensional materials has greatly improved in recent years. Since the synthesis of graphene,[1,2] a large number of extensive systems only a few atoms thick have been obtained. The study of these 2D materials has brought new physical phenomena with countless applications into play, like their magnetic properties.[3,4] Obtaining magnetism in 2D isotropic crystals is forbidden in the Heisenberg model as explained by the Mermin–Wagner theorem:[5] the magnon dispersion is reduced with respect to their 3D counterparts, and it has an abrupt onset, which translates into low thermal agitation and a collapse of the spin order. However, 2D systems with uniaxial magnetic anisotropy are able to withstand thermal agitation, allowing magnetic states in mono and multilayer materials.

In the past few decades, the study of 2D magnetic properties has been performed on epitaxially grown thin films, in which phenomena such as oscillatory exchange coupling,[6,7] giant magnetoresistance[8,9] and the Hall effect[10,11] have been observed. Nevertheless, the study of the intrinsic magnetic properties of these 2D systems is novel, and most of the materials that have been synthesized are magnetic van der Waals crystals.[3,4,12,13] In the last five years, non-van der Waals two-dimensional materials have also been synthesized, mainly by exfoliating naturally occurring ores. By liquid exfoliation of natural iron ore hematite (α-Fe_2O_3), Balan *et al.*[14] synthesized a new 2D material called hematene. In contrast to its antiferromagnetic bulk, hematene presents ferromagnetic order.[15] Similarly, another promising material for 2D magnets is ilmenene,[16] which has been synthesized using liquid phase exfoliation from titanate ore ilmenite ($FeTiO_3$). Motivated by the synthesis of iron ilmenene, other similar 2D materials could be exfoliated from the bulk systems with their 3D counterpart ilmenite-like structures.

The aim of the present work is thus to characterize ilmenene-like titanates ($TMTiO_3$, TM = V to Zn) to set the first theoretical basis for this exciting family of materials. Within the framework of density functional theory, we systematically analyze the crystalline structure of these compounds, finding that most of the ilmenenes exhibit triangular symmetry for TMs on both sides of a Ti–Ti hexagonal graphene-like sublattice. In the chromium and copper ilmenenes, we find structural distortions of Jahn–Teller origin. Our electronic structure calculations reveal that most of these compounds are magnetic semiconductors which have TM layers that are antiferromagnetically coupled. The calculations including the spin–orbit interaction show a strong magnetic anisotropy, with the magnetization being oriented out-of-plane (in-plane) below (above) half-filling of the TM electronic 3d shell. The presence of out-of-plane anisotropy in some of these compounds suggests potential applications for spintronics in thin layers and 2D materials.

[a]*Donostia International Physics Center (DIPC), 20018 Donostia, Spain. E-mail: a.ayuela@csic.es*

[b]*Centro de Física de Materiales – Materials Physics Center (CFM-MPC), 20018 Donostia, Spain*

[c]*EHU Quantum Center, Universidad del País Vasco/Euskal Herriko Unibertsitatea UPV/EHU, Leioa, Spain*

† Electronic supplementary information (ESI) available. See DOI: https://doi.org/10.1039/d3na00134b

2 Model details

In this work, we study the structural, electronic and magnetic properties of ilmenene-type materials using the projector augmented wave method (PAW) implemented in the Vienna *Ab initio* Software Package (VASP).[17,18] For the exchange and correlation potential we use the Perdew–Burke–Ernzerhof form of the generalized gradient approximation (GGA), with the formulation of Dudarev[19] for GGA + *U*. The Hubbard *U* parameters for each element are chosen based on the available literature on transition metal oxides,[20] and are shown in Table S1 of the ESI† with the considered valence states. A test calculation of the partial density of states (PDOS) of cobalt titanate using the HSE06 hybrid functional shows that including a *U* parameter in the oxygen p-orbitals is needed to correctly describe the electronic structure. This finding is in agreement with previous investigations concerning titanium oxide and hematite.[21–26] All calculations are performed with a well-converged plane-wave cutoff energy of 800 eV, a gamma-centered $4 \times 4 \times 1$ Monkhorst–Pack *k*-point mesh, and a Fermi smearing of 20 meV. Atomic coordinates are relaxed until forces in all directions are smaller than 0.5 meV $Å^{-1}$. An energy convergence criterion of 10^{-7} eV is used. Further tests using even a larger plane wave cutoff up to 1000 eV and $6 \times 6 \times 1$ *k*-point mesh do not modify the presented results. Differences in local charges and local magnetic moments are univocally analyzed using the Bader method.[27,28] By including the spin–orbit coupling, additional tests are performed to converge the magnetocrystalline anisotropy energy with respect to the Brillouin zone sampling.

The d-metal ilmenene sheets are obtained by cutting their respective bulk titanates ($TMTiO_3$, TM = V to Zn) in the hexagonal [001] direction. For the iron ilmenene $FeTiO_3$, transmission electron microscopy measurements confirm the 2D structure in this direction.[16] The layer structure is shown in Fig. 1. For all the compounds under analysis, two different layer-ilmenenes are tested: titanium and transition metal terminated ilmenene layers. This work focuses on the TM ended layers because they are found to be more stable for all the materials under analysis.

3 Results and discussion

3.1 Structural properties

The structure of the TM ilmenenes is graphically depicted from two viewpoints in Fig. 1. After structural relaxations, we find that most of the compounds keep the input symmetry, except for chromium and copper ilmenenes, which show structural deformations of the perfect lattice due to the Jahn–Teller effect (see Fig. 1(b)). The orange area in panel (a) denotes the chemical cell that reproduces the crystalline structure of the ilmenenes when periodically repeated. We calculate magnetic configurations using a larger $2 \times 2 \times 1$ magnetic cell. For chromium and copper titanates, due to structural distortions, the unit cell and the magnetic cell coincide. In the distorted compounds, the two in-plane lattice vectors become slightly different: for the chromium case $a = 10.57$ Å and $b = 10.00$ Å, and for the copper case $a = 10.44$ Å and $b = 10.21$ Å. Note that these ilmenenes become anisotropic. Overimposed on the global lattice distortions, the inner atomic distortions become more noticeable. For instance, the largest–smallest distances are 6.0–3.9 Å and 5.4–4.8 Å for Cr and Cu ilmenenes, respectively. The large 1D anisotropy of these two Jahn–Teller distorted ilmenenes is shown by the stripes of the green and violet areas in Fig. 1(b).

A summary of the interatomic distances of the TM titanates is shown as a function of the elements across the period in the periodic table in Fig. 1. We find that the horizontal distance between transition metals in the same layer l_{TM-TM} increases from V to Mn, then decreases until Ni, and finally increases for the brass metals Cu and Zn. The height distance between metals in different layers h_{TM-TM} generally decreases. The distances involving Ti in the Ti–Ti and Ti–O bonds remain nearly constant, while the TM–O distances decrease. In essence, TM-ilmenenes can be thought of as a solid network formed by Ti and O atoms on which the TM atoms attach on both sides. For the Cr and Cu ilmenenes showing structural distortions, the TM–TM distances have two values because the triangular symmetry is broken, and the Ti–O distances are split into several values as shown by the extra marks in the lower panel of Fig. 1.

We find that in comparison with their bulk counterparts, TM ilmenenes are compacted along the *c* direction, so that a two-dimensional hexagonal layer of titanium ions is formed similar to graphene. The Ti–Ti sublattice in ilmenenes remains almost constant with the distances varying within 3%.‡ This compression for the iron ilmenene has a minimum height of about 2.91 Å, in agreement with another work.[16] The theoretical value of 2.59 Å for the interplanar space corresponding to the $(11\bar{2}0)$ and $(\bar{2}110)$ lattice spacing compares well with the experimental one (~2.53 Å),[16] which also supports our calculations since the interatomic distances depend on the chosen *U* values. For cobalt titanates, a layer thickness of 4.03 Å has been reported[29] in bulk, which decreases to 2.95 Å in the ilmenene layer, while the horizontal distance between cobalt atoms in the same layer expands slightly from 5.06 Å in the bulk to 5.17 Å in the layer. The significant changes in the height distances are due to the layer being decorated with half of the TM atoms in the corresponding bulk, in order to keep the stoichiometry. The ilmenene layers differ greatly from those found in ilmenites and thus not only their structural properties but also their magnetic ones deserve a thorough study.

Dynamics stability is mainly based on the calculation of phonons. These phonons for the iron case were calculated by Balan *et al.*[16] and show that these structures are stable. Note that the ilmenene structures have also been found experimentally. For V, Mn, Fe, Ni and Zn ilmenenes, we calculate the frequencies at $q = 0$ and to an accuracy of 0.0001 cm^{-1} they are positive and do not see any negative frequency. In addition, these ilmenenes are chemically stable because they show non-negligible gaps. In fact, we are performing relaxations without symmetry, and in some cases like chromium and copper ilmenenes get distorted from the perfect symmetry into other

‡ However, the chromium titanate layer does not show the fully compacting behavior of a flat titanium sheet (see Fig. 1(b)).

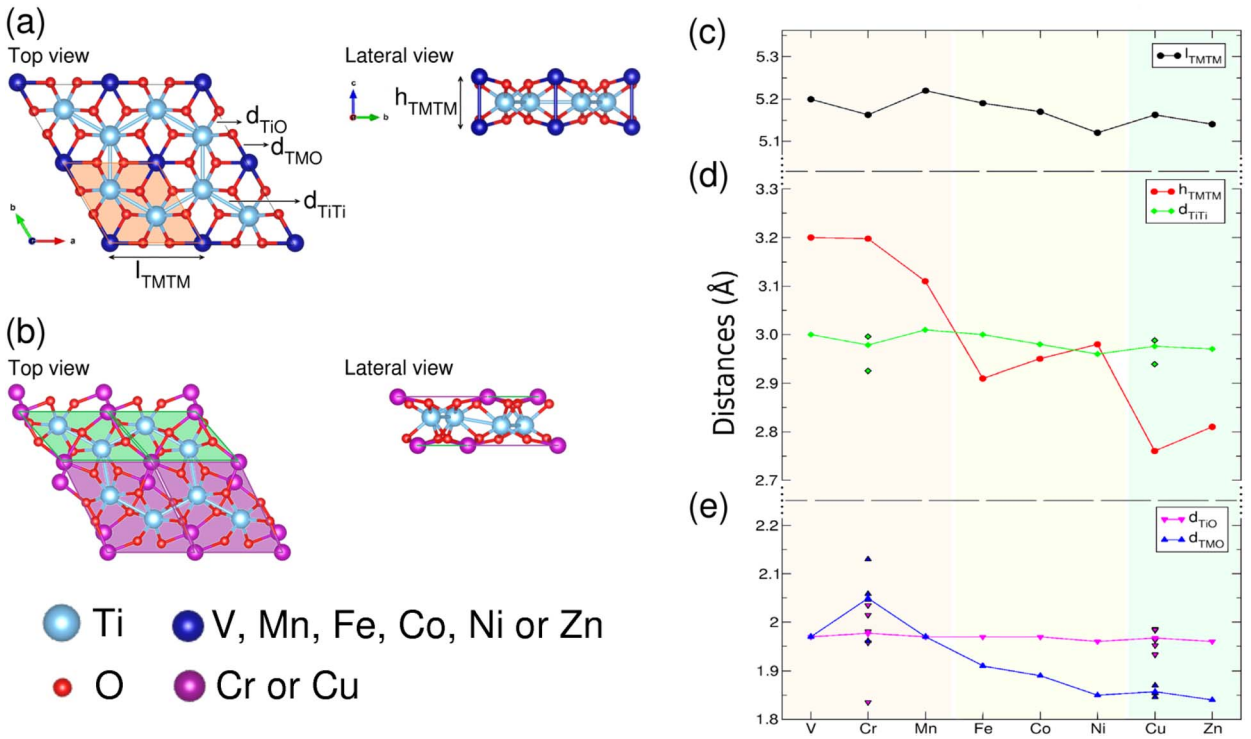

Fig. 1 Magnetic unit cell for transition metal ended ilmenene-like systems: (a) symmetric for most ilmenenes and (b) distorted for chromium titanate $CrTiO_3$. The color code of the atoms is as follows: TM (Cr) atoms in blue (purple), titanium in cyan, and oxygen in red. The orange area in panel (a) represents the smaller chemical cell. For chromium and copper titanates, the chemical and magnetic cells coincide. Calculated interatomic distances: (c) horizontal TM–TM distance l_{TM-TM}, (d) layer height h_{TM-TM} and Ti–Ti distances, and (e) Ti–O and TM–O distances. For the chromium and copper ilmenenes we present an average of the distances in their distorted structures.

structures, having also gaps. Summing up it seems that these compounds are indeed structurally stable.

3.2 Electronic properties: magnetic semiconductors

We now focus on the electronic structure of ilmenenes and find that they show a gap opening that is linked to their stability. The calculated electronic band gaps range between 1.8 and 4 eV, as displayed in Fig. 2(a), with the values being typical of semiconductors. All the layers studied here show a gap indicating that they are chemically stable. The gaps are increasing when going from V to Mn, and they are oscillating for Fe, Co and Ni. In general, the values are smaller than the gap for TiO_2 in the rutile bulk phase (~3.2 eV). Note that the Mn and the Co ilmenenes remain within the same order of the TiO_2 gap values. These trends follow the filling of 3d TM electronic levels as discussed below.

The TM atoms in the ilmenene compounds show local magnetic moments, which are calculated using the Bader method, and are shown in panel (b) of Fig. 2. The calculated values are close to the ones expected by applying the Hund rules to isolated ions. Furthermore, the local magnetic moment as a function of atomic number follows a Slater–Pauling-like rule, increasing from vanadium to manganese, then decreasing until it vanishes for zinc. Thus, the 3d ilmenenes can be taken as magnetic semiconductors.

The band structures and the PDOS projected onto the transition metal atoms are provided in the ESI.† From their analysis, an electronic filling model for each TM ilmenene is presented in Fig. 2(b). We find that the orbitals can be classified into three groups: (i) out-of-plane d_{z^2}, (ii) in-plane $d_{x^2-y^2}$ and d_{xy}, and (iii) mixing in- and out-of-plane contributions for d_{xz} and d_{yz}. The $d_{x^2-y^2}$ and d_{xy} orbitals are highly hybridized, as the d_{xz} and d_{yz} orbitals are. Because the in-plane degenerate energy levels of chromium and copper titanates are being partially occupied, they are held responsible for the Jahn–Teller-like distortions in these structures, where a splitting of these otherwise degenerate orbitals is observed under distortions.

All these electronic trends can be better understood following the density in real space for each case around the transition and brass metals by considering the occupation and shape of the orbitals in 3D, as shown in Fig. 2(c). Below half-filling, we show how the magnetic moment increases in correlation with the gap values. For the next elements, above half-filling, the Fe case becomes similar to the Ni one which has a weaker spin distribution. In between, we find the Co ilmenene with a large in-plane spin distribution, also having an out-of-plane component that cannot be neglected, an extra component that is related to the complexity added to this case when trying to write down a single spin Hamiltonian. For brass metals, the local magnetization is nearly screened having a spin compensated cloud around the brass metal centers. This model

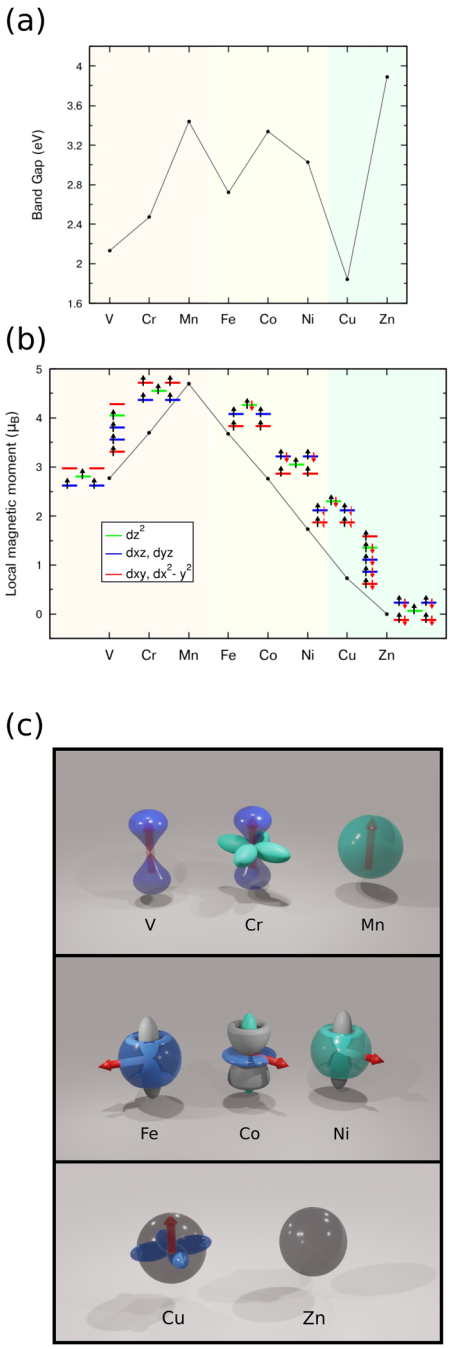

Fig. 2 (a) Electronic band gaps for TM ilmenenes. Vertical lines separate different regions with TM below half-filling, TM above half-filling, and brass metals. (b) Calculated local magnetic moment around transition metal atoms. For each compound, the electronic filling model of the ground state is also shown. Red levels represent the in-plane $d_{x^2-y^2}$ and d_{xy} orbitals; green, the out-of-plane d_{z^2} orbital; and blue, the d_{xz} and d_{yz} orbitals with in- and out-of-plane components. (c) 3D models of the density around atoms in 3d TMs and brass metals within ilmenenes. Blue and green regions denote spin polarized regions; grey denotes spin compensated ones.

is going to be interesting in the discussion of magnetic anisotropy below. For instance, we note that the spin distribution is anisotropic in-plane for the case of Cr (Cu) having one electron less below a half-filled (filled) 3d shell.

3.3 Magnetic ordering

We next consider the magnetic behavior of the ilmenene-type materials, and calculate the total energies of the magnetic configurations shown schematically in Fig. 3. We find that, with the exception of ferromagnetic copper and spin-compensated zinc titanates, the ilmenenes show antiferromagnetism between the 2D TM layers in the so-called AFM-1 configuration. The magnetic configurations in Fig. 3 are used to fit the Heisenberg Hamiltonian

$$H = -\sum_{ij} J_{ij} \tilde{S}_i \tilde{S}_j \quad (1)$$

where $\tilde{S}_i$ is the pseudospin of each isolated atomic species (*e.g.*: $\tilde{S} = 3/2$ for Co) and the J_i with $i = 1, 2$ are the inter-layer ($i = 1$) and intra-layer ($i = 2$) magnetic couplings schematically depicted in Fig. 3. The magnetic couplings are computed from the energy differences $\Delta E_1 = E_{\mathrm{FM}} - E_{\mathrm{AFM1}}$ and $\Delta E_2 = E_{\mathrm{AFM2}} - E_{\mathrm{AFM1}}$.

The fitted J_i values are shown in Fig. 3(b). The inter-layer coupling is the leading interaction because J_1 is an order of magnitude larger than J_2. The inter-layer coupling J_1 is negative for most of the ilmenenes, which indicates a preference for antiferromagnetism. The intralayer coupling J_2 is positive in all cases, and the compounds favor intralayer ferromagnetism. Since the coordination of the TM atoms on each layer side changes from being hexagonal in the bulk to triangular in the layer, the structural differences between the bulk and two-dimensional titanates mentioned above play an important role in the magnetic ordering. It is noteworthy that the manganese ilmenene even favors ferromagnetism within layers in contrast with its antiferromagnetic bulk counterpart.

3.4 Magnetic anisotropy

We last study the magnetic anisotropy of d-metal ilmenenes. The spin–orbit interaction couples the spin magnetic moment to the crystal lattice, which means that some spin orientations are more stable than others. The magnetocrystalline anisotropy energy (MAE) is defined as the energy difference between two magnetic configurations with different spin orientations. We calculate the total energy of the ilmenenes for a number of spin orientations, and find that, anisotropy-wise, ilmenenes can be classified into two groups: out-of-plane ilmenenes, in which the spin magnetic moment is aligned in the *c*-axis, and in-plane ilmenenes, with the spin aligned in any of the directions along TM–Ti bonds projected in the plane (see Fig. 4). Due to the symmetry around TM atoms, there are six such equivalent directions in the *ab* plane. The vanadium, chromium and manganese titanates in addition to copper ones have an out-of-plane anisotropy, and the magnetization in iron, cobalt and nickel titanates is oriented in-plane. These MAE trends agree with the electronic filling model, in which for below half-filling TMs the electrons near the Fermi level are those that include an out-of-plane component, and for iron, cobalt and nickel titanates they are mainly in-plane.

The obtained MAE values range between several orders of magnitude from 10^{-2} meV up to tenths of meVs because the

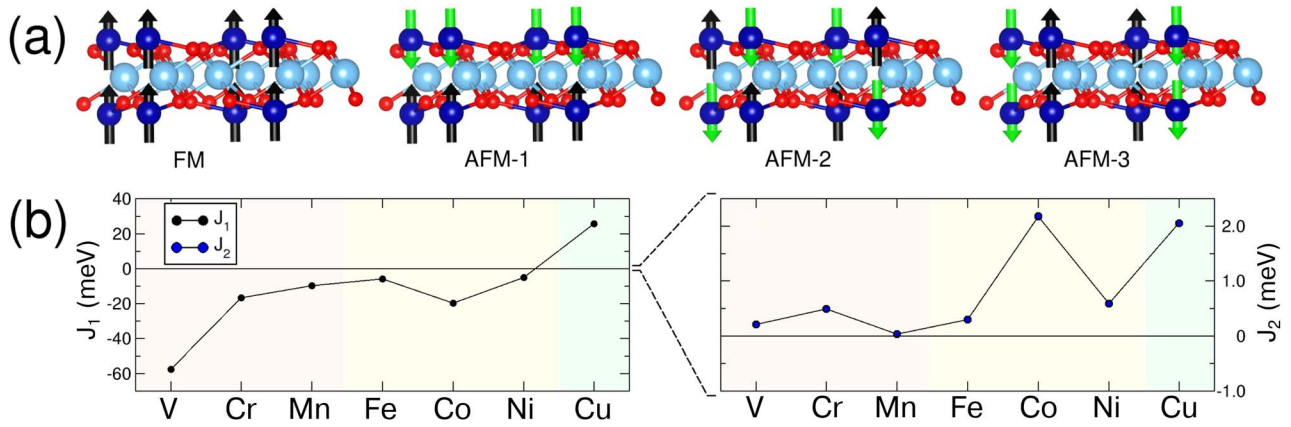

Fig. 3 (a) Magnetic ordering configurations of TM ilmenenes: "FM" ferromagnetic, "AFM-1" antiferromagnetic by layers, "AFM-2" and "AFM-3" antiferromagnetic. (b) Couplings between both layer sides (J_1), and within the same side layer of TM ions (J_2).

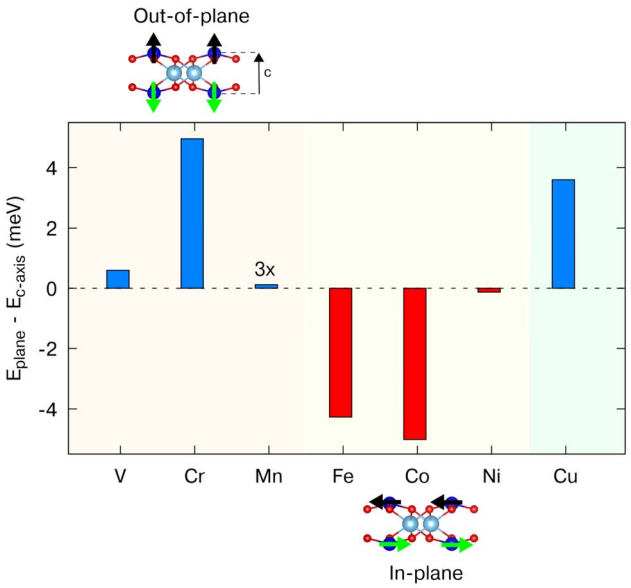

Fig. 4 Magnetocrystalline anisotropy energy of the transition metal ilmenenes. In blue, compounds with out-of-plane anisotropy; in red, with in-plane magnetic moments. For the case of manganese titanate, the magnitude was enhanced by a factor of 3 to make it visible in the shown range.

spin–orbit interaction varies greatly for the different ilmenenes. The chromium, iron and cobalt titanates have a strong MAE of around 5 meV, and in the case of the vanadium and nickel layers, this value is still large, about 0.6 and 0.13 meV, respectively. The manganese titanate has the smallest anisotropy (~0.04 meV) because the orbital magnetic moment is nearly fully quenched. This finding that the energy difference between the magnetic AFM-1 and AFM-2 configurations of the manganese titanate is very small (around 0.25 meV) points to non-collinear magnetic configurations, a topic that might merit future experimental investigation on this specific layer, but is beyond the actual scope of the paper. Furthermore, the cobalt ilmenene is also a particular 2D layer because it shows a strong in-plane anisotropy, in contrast to the theoretical ilmenite bulk with a non-negligible out-of-plane component.

We observe a noticeable trend for the magnetic anisotropy. Below half-filling, the V and Cr ilmenenes exhibit out-of-plane anisotropy, while the half-filled manganese ilmenene has a very small MAE. Above half-filling, most the compounds have an in-plane anisotropy. In fact, these trends in anisotropy follow the levels depicted in Fig. 2(c). For V and Cr ilmenenes, it shows that the spin density is perpendicular to the plane. The spin density in manganese ilmenene is isotropic, and this correlates with its low MAE. Above half-filling, the spin density of Fe, Co and Ni ilmenenes lies in-plane, in agreement with their in-plane MAE. The case of Cu ilmenene shows out-of-plane anisotropy even if the spin density lies in-plane, a finding that can be explained by the out-of-plane changes in the orbitals when the spin–orbit coupling term is included with the distortions.

We next bring together the magnetic results on magnetic ilmenenes with experimental facts. Note that Fe ilmenenes can be obtained by exfoliation and deposited on substrates for some experimental setups.[14,16] Then, further measurements on the magnetic properties of the Fe ilmenenes can be today performed in line with our theoretical results. Furthermore, we have studied Co ilmenenes that could be interesting as they can behave in a similar way to study magnon physics in two dimensions as their bulk counterpart is already being used.[29–31] In fact, Cr ilmenenes seem to become key as they are candidates to show out-of-plane anisotropy when in the form of ultrathin layers. These findings suggest the future use of TM ilmenenes in spintronics devices for injecting magnons and studying magnetism in exfoliated 2D magnetic layers.

4 Conclusions

In this work, we have analyzed the structural, electronic and magnetic properties of TM ilmenene-like systems. Our calculations reveal that most of the materials under analysis present a triangular crystalline structure for TMs, with an ironed compression of the internal titanium ion layer with respect to the bulk. The chromium and copper ilmenenes exhibit notable

structural distortions, which seem to have a Jahn–Teller origin. All the compounds studied have been found to be magnetic semiconductors with band gaps in the range between 1.7 and 4 eV. The magnetic ground state is mainly antiferromagnetic between layers, and ferromagnetic and spin-compensated for $CuTiO_3$ and $ZnTiO_3$, respectively. Furthermore, spin–orbit calculations revealed that TM ilmenenes can be divided into two groups: out-of-plane ilmenenes, for less than half-filling of the 3d bands, and in-plane ilmenenes, for above half-filling of these levels, with the spin aligned in the TM–titanium directions projected in the hexagonal plane. We believe that this family of materials paves the way to other types of promising 2D candidates with potential applications in the field of spintronics. Note that we expand the previous studies to consider other transition metals in ilmenenes, so certainly the paper is not within expectations. There is novelty in the data because the iron ilmenenes are in fact behaving differently from others. For instance, study on the magnetic anisotropy was missing even for the iron ilmenene in a previous reference. The iron ilmenene shows magnetic anisotropy, that is, being in-plane, and behaves differently from other ilmenenes with transition and brass metals, that is, being out-of-plane. Furthermore, it is noteworthy that the calculated magnetic properties of ilmenenes are different from those found in bulk ilmenites.

Conflicts of interest

There are no conflicts to declare.

Acknowledgements

This work has been supported by the Spanish Ministry of Science and Innovation through grants PID2019-105488GB-I00, TED2021-132074B-C32 and PCI2019-103657. We acknowledge financial support by the European Commission from the MIRACLE (ID 964450), NaturSea-PV (ID 101084348), and NRG-STORAGE project (GA 870114). The Basque Government supported this work through Project No. IT-1569-22. M. A. was supported by the Spanish Ministry of Science and Innovation through the FPI PhD Fellowship BES-2017-079677. R. H. A.-T. acknowledges the postdoctoral contract from the Donostia International Physics Center.

Notes and references

1 K. S. Novoselov, A. K. Geim, S. V. Morozov, D. Jiang, Y. Zhang, S. V. Dubonos, I. V. Grigorieva and A. A. Firsov, *Science*, 2004, **306**, 666–669.
2 A. K. Geim and K. S. Novoselov, *Nat. Mater.*, 2007, **6**, 183–191.
3 C. Gong, L. Li, Z. Li, H. Ji, A. Stern, Y. Xia, T. Cao, W. Bao, C. Wang, Y. Wang, *et al.*, *Nature*, 2017, **546**, 265–269.
4 B. Huang, G. Clark, E. Navarro-Moratalla, D. R. Klein, R. Cheng, K. L. Seyler, D. Zhong, E. Schmidgall, M. A. McGuire, D. H. Cobden, *et al.*, *Nature*, 2017, **546**, 270–273.
5 N. D. Mermin and H. Wagner, *Phys. Rev. Lett.*, 1966, **17**, 1133–1136.
6 K. R. Nikolaev, A. Y. Dobin, I. N. Krivorotov, W. K. Cooley, A. Bhattacharya, A. L. Kobrinskii, L. I. Glazman, R. M. Wentzovitch, E. D. Dahlberg and A. M. Goldman, *Phys. Rev. Lett.*, 2000, **85**, 3728–3731.
7 R. R. Gareev, D. E. Bürgler, M. Buchmeier, D. Olligs, R. Schreiber and P. Grünberg, *Phys. Rev. Lett.*, 2001, **87**, 157202.
8 M. N. Baibich, J. M. Broto, A. Fert, F. N. Van Dau, F. Petroff, P. Etienne, G. Creuzet, A. Friederich and J. Chazelas, *Phys. Rev. Lett.*, 1988, **61**, 2472–2475.
9 G. Binasch, P. Grünberg, F. Saurenbach and W. Zinn, *Phys. Rev. B: Condens. Matter Mater. Phys.*, 1989, **39**, 4828–4830.
10 X. W. Li, A. Gupta, T. R. McGuire, P. R. Duncombe and G. Xiao, *J. Appl. Phys.*, 1999, **85**, 5585–5587.
11 J. M. Taylor, A. Markou, E. Lesne, P. K. Sivakumar, C. Luo, F. Radu, P. Werner, C. Felser and S. S. P. Parkin, *Phys. Rev. B*, 2020, **101**, 094404.
12 B. Huang, G. Clark, D. Klein, D. MacNeill, E. Navarro-Moratalla, K. Seyler, N. Wilson, M. McGuire, D. Cobden, X. di, W. Yao, P. Jarillo-Herrero and X. Xu, *Nat. Nanotechnol.*, 2018, **13**, 544–548.
13 A. Leon, J. González, F. Crasto de Lima, J. Mejia-Lopez and E. Suarez Morell, *2D Materials*, 2020, **7**, 035008.
14 A. Puthirath Balan, S. Radhakrishnan, C. F. Woellner, *et al.*, *Nat. Nanotechnol.*, 2018, **13**, 602–609.
15 R. Gonzalez, J. Mella Riquelme, P. Díaz, S. Allende, E. Vogel, C. Cardenas and F. Munoz, *2D Materials*, 2019, **6**, 045002.
16 A. Puthirath Balan, S. Radhakrishnan, R. Kumar, R. Neupane, S. K. Sinha, L. Deng, C. A. de los Reyes, A. Apte, B. M. Rao, M. Paulose, R. Vajtai, C. W. Chu, G. Costin, A. A. Martí, O. K. Varghese, A. K. Singh, C. S. Tiwary, M. R. Anantharaman and P. M. Ajayan, *Chem. Mater.*, 2018, **30**, 5923–5931.
17 G. Kresse and J. Furthmüller, *Phys. Rev. B: Condens. Matter Mater. Phys.*, 1996, **54**, 11169–11186.
18 G. Kresse and D. Joubert, *Phys. Rev. B: Condens. Matter Mater. Phys.*, 1999, **59**, 1758–1775.
19 S. L. Dudarev, G. A. Botton, S. Y. Savrasov, C. J. Humphreys and A. P. Sutton, *Phys. Rev. B: Condens. Matter Mater. Phys.*, 1998, **57**, 1505–1509.
20 F. Aguilera-Granja and A. Ayuela, *J. Phys. Chem. C*, 2020, **124**, 2634–2643.
21 S. Lany, *J. Phys.: Condens. Matter*, 2015, **27**, 283203.
22 S. Lany, H. Raebiger and A. Zunger, *Phys. Rev. B: Condens. Matter Mater. Phys.*, 2008, **77**, 241201.
23 B. J. Morgan and G. W. Watson, *Phys. Rev. B: Condens. Matter Mater. Phys.*, 2009, **80**, 233102.
24 X. Huang, S. K. Ramadugu and S. E. Mason, *J. Phys. Chem. C*, 2016, **120**, 4919–4930.
25 L. Jiang, S. V. Levchenko and A. M. Rappe, *Phys. Rev. Lett.*, 2012, **108**, 166403.
26 G. Y. Gou, J. W. Bennett, H. Takenaka and A. M. Rappe, *Phys. Rev. B: Condens. Matter Mater. Phys.*, 2011, **83**, 205115.
27 W. Kutzelnigg, *Angew. Chem., Int. Ed. Engl.*, 1993, **32**, 128–129.
28 G. Henkelman, A. Arnaldsson and H. Jónsson, *Comput. Mater. Sci.*, 2006, **36**, 354–360.

29 M. Arruabarrena, A. Leonardo, M. Rodriguez-Vega, G. A. Fiete and A. Ayuela, *Phys. Rev. B*, 2022, **105**, 144425.
30 M. Elliot, P. McClarty, D. Prabhakaran, R. Johnson, H. Walker, P. Manuel and R. Coldea, *Nat. Commun.*, 2021, **12**, 3936.
31 B. Yuan, I. Khait, G.-J. Shu, F. C. Chou, M. B. Stone, J. P. Clancy, A. Paramekanti and Y.-J. Kim, *Phys. Rev. X*, 2020, **10**, 011062.